

Transport in molecular states language: Generalized quantum master equation approach

Massimiliano Esposito^{1,*} and Michael Galperin¹

¹*Department of Chemistry & Biochemistry, University of California San Diego, La Jolla CA 92093, USA*

(Dated: September 15, 2021)

A simple scheme capable of treating transport in molecular junctions in the language of many-body states is presented. An ansatz in Liouville space similar to generalized Kadanoff-Baym approximation is introduced in order to reduce exact equation-of-motion for Hubbard operator to quantum master equation (QME)-like expression. A dressing with effective Liouville space propagation similar to standard diagrammatic dressing approach is proposed. The scheme is compared to standard QME approach, and its applicability to transport calculations is discussed within numerical examples.

PACS numbers: 85.65.+h 85.35.Be 73.63.Kv 73.23.Hk

I. INTRODUCTION

Quantum transport in nanoscale systems is on the forefront of research in many fields of study. In particular, progress of experimental capabilities in the field of molecular electronics brings new theoretical challenges.¹ Resonant transport with strong on-the-bridge interactions is one of them. It is probably the most important regime for possible future applications (e.g. for logic and memory molecular devices). Unlike usual mesoscopic systems, molecular electronic (and vibrational) structure may be very sensitive to reduction/oxidation. Thus resonant transport in molecular junctions has to be described in the language of molecular states (states of the isolated molecule as a basis for description of reduced non-equilibrium dynamics), rather than in the language of (effective) single-particle orbitals, which is generally accepted in the molecular electronics community. Recent experiments on simultaneous measurements of current and optical response of molecular junctions² make need for such formulation even more pronounced, since molecular states is a natural language of all the (equilibrium) molecular spectroscopy. Besides, molecular states based formulation of transport makes it potentially possible to incorporate standard quantum chemistry molecular structure simulations as an input to transport calculations.

Necessity of many-body states type description of transport in molecular systems has been realized. Among the approaches one can mention scattering theory,³ (generalized) master equation,^{4,5,6,7,8,9} density matrix,^{10,11,12,13,14,15,16} and non-equilibrium Green function (NEGF) based schemes.^{19,20,21} Each of these schemes has its own limitations. Scattering theory when applied to transport problems disregards junction character of molecular system which may lead to erroneous predictions.^{17,18} Standard formulations also miss crucial physics, e.g. effective attractive electron-electron interaction via phonons (bipolaron formation), energy exchange (heating and cooling effects) between successive tunneling events, target distortion due to quasi-bound states etc. Master equation (or generalized master equa-

tion) approaches are used quite often to describe hopping transport, i.e. situation when correlations in the system (both in space and time) die much quicker than electron transfer time (fixed by contact/molecule coupling). Besides, they become inadequate in the off-resonant tunneling (super-exchange) situation. Density matrix schemes usually formulated within quantum master equation form, often miss broadening of molecular states due to coupling to the contacts and coherences responsible, e.g., for elastic channel renormalization at the inelastic threshold (see also discussion below). NEGF based approaches in the language of molecular states are among the most advanced methods for treating non-equilibrium molecular systems.²¹ Two important drawbacks of the approach are its complicated character and absence of proper commutation relations for the Hubbard operators. The first means that applicability of the method is limited to simple cases only. The second may lead to unphysical consequences (e.g. non-Hermiticity of the reduced density matrix) at approximate level of treatment.^{22,23}

The goal of the present paper is to formulate an approximate scheme for treatment of transport in molecular junctions in the language of molecular states, exploring connection between Green function and density matrix based approaches to transport. We start from the NEGF-like consideration and derive QME-like equation, pointing out approximations involved in the derivation. Note that similar approach within a single-particle orbitals language was used in Ref. 24. Note also that in our consideration we go beyond strictly Markov limit of Ref. 13. We work with Hubbard operator as a natural object capable of describing excitation in the molecule as transitions (we restrict our consideration to single-electron transitions) between many-body molecular states. First we show how exact equation can be reduced to QME by introducing ansatz in Liouville space similar to the generalized Kadanoff-Baym approximation (GKBA)²⁵ in Hilbert space. Second, we identify diagrams on the Keldysh contour corresponding to the processes described by QME, and in the spirit of Green function diagrammatic techniques dress this diagrams

arXiv:0811.4014v1 [cond-mat.mes-hall] 25 Nov 2008

by effective Liouville space dynamics. The last is obtained from the exact equation within Markov approximation. Section II introduces molecular junction model and presents equation-of-motion for the Hubbard operator. In section III we introduce an ansatz in the Liouville space, which being similar to the GKBA, allows reduction of the exact EOM for the Hubbard operator to QME. Here we also discuss a dressing procedure. Section IV presents analytical consideration for the simple resonant level model, and discuss general numerical procedure. Several numerical examples are presented as well. Section V concludes.

II. MODEL

We consider molecular junction which consists of two contacts (L and R) coupled through the molecule (M). Contacts are assumed to be reservoirs of free electrons each at its own equilibrium. All the non-equilibrium physics takes place at the molecule. Hamiltonian of the system is

$$\hat{H} = \hat{H}_L + \hat{H}_M + \hat{H}_R + \hat{V} \equiv \hat{H}_0 + \hat{V} \quad (1)$$

where \hat{H}_M is a full molecular Hamiltonian, i.e. Hamiltonian of isolated molecule with all on-the-molecule interactions included, \hat{V} is molecule-contacts coupling

$$\hat{V} = \sum_{m \in M, k \in \{L, R\}} \left(V_{km} \hat{c}_k^\dagger \hat{d}_m + V_{mk} \hat{d}_m^\dagger \hat{c}_k \right) \quad (2)$$

and \hat{H}_K ($K = L, R$) represents contacts

$$\hat{H}_K = \sum_{k \in K} \varepsilon_k \hat{c}_k^\dagger \hat{c}_k \quad (3)$$

Here c_k^\dagger (\hat{c}_k) and d_m^\dagger (\hat{d}_m) are creation (annihilation) operators for electron in a state k in contact K and state m of molecular Hamiltonian, respectively.

We introduce many-body states of isolated molecule $|N, i\rangle$ with N being number of electrons on the molecule and i standing for a set of all other quantum numbers characterizing particular state of the molecule in the charging block N . These states are assumed to be orthonormal

$$\langle N, j | N', i' \rangle = \delta_{N, N'} \delta_{i, i'} \quad (4)$$

Note, that generalization to nonorthogonal basis is available in the literature,²⁶ but we will stick with orthonormal basis in order to keep notation as simple as possible. Molecular transitions (in our case due to coupling to the contacts) are naturally described in the language of Hubbard operators

$$\hat{X}_{(N, i; N', i')} = |N, i\rangle \langle N', i'| \quad (5)$$

One of important (in our case) transitions is oxidation/reduction of the molecule by one electron, i.e. transition between neighboring charge blocks

$$\mathcal{M} \equiv (N, i; N+1, j) \quad \bar{\mathcal{M}} \equiv (N+1, j; N, i) \quad (6)$$

In terms of these states molecular Hamiltonian is

$$\hat{H}_M = \sum_{N, i, j} |N, i\rangle \langle N, j| H_{ij}^{(N)} \equiv \sum_{N, i, j} H_{ij}^{(N)} \hat{X}_{(N, i; N, j)} \quad (7)$$

If the many-body states are chosen to be eigenstates of the molecular Hamiltonian, $H_{ij}^{(N)} = E_i^{(N)} \delta_{i, j}$ with $E_i^{(N)}$ being energy of the molecular eigenstate $|N, i\rangle$. Molecule-contacts coupling, Eq.(2), becomes

$$\hat{V} = \sum_{k, \mathcal{M}} \left(V_{k\mathcal{M}} \hat{c}_k^\dagger \hat{X}_{\mathcal{M}} + V_{\bar{\mathcal{M}}k} \hat{X}_{\bar{\mathcal{M}}} \hat{c}_k \right) \quad (8)$$

where

$$V_{k\mathcal{M}} \equiv \sum_{m \in M} V_{km} \langle N, i | \hat{d}_m | N+1, j \rangle \quad (9)$$

and $V_{\bar{\mathcal{M}}k} \equiv V_{k\mathcal{M}}^*$. Note, that $\hat{X}_{\bar{\mathcal{M}}} = \hat{X}_{\mathcal{M}}^\dagger$.

In our previous publication,²¹ we considered application of a method originally formulated in Ref. 19, to inelastic transport in molecular junctions. The main object of interest in this consideration was many-body (Hubbard) Green function on the Keldysh contour

$$G_{(a;b),(c;d)}(\tau, \tau') \equiv -i \langle T_c \hat{X}_{ab}(\tau) \hat{X}_{cd}^\dagger(\tau') \rangle \quad (10)$$

where a, b, c, d are many-body states of an isolated molecule, T_c is the contour ordering operator, and τ, τ' are contour variables. The consideration leads to a formulation similar to standard diagrammatic technique, with series of functional derivatives in place of expansion in small parameter for conventional diagrammatic consideration (for a detailed discussion see Ref. 21). Thus obtained machinery is quite general, but may be too heavy for realistic applications. Also at approximate level of treatment it may lead to non-physical results.^{22,23}

Here the main object of interest will be the operator $\hat{X}_{ab}(t) = e^{i\hat{H}t} \hat{X}_{ab} e^{-i\hat{H}t}$, where $|a\rangle \equiv |N_a, s_a\rangle$ and $|b\rangle \equiv |N_b, s_b\rangle$ are many-body states defined in (4), and t is time. Our goal is utilizing Green function techniques find a (approximate) connection to density matrix based considerations (in a manner similar to that of Ref. 27), and use resulting scheme as a simplified version of a procedure considered in e.g. Ref. 21. Note, that we are going to go beyond standard QME considerations of transport (see discussion below). Our starting point is EOM

$$\frac{d \langle \hat{X}_{ab}(t) \rangle}{dt} = i \left\langle \left[\hat{H}; \hat{X}_{ab}(t) \right] \right\rangle \quad (11)$$

Taking commutator in the right side of (11) yields correlation functions of the form (for detailed derivation see

Appendix A) $\langle \hat{X}_{(\dots)}^\dagger(t) \hat{c}_k(t) \rangle$ and $\langle \hat{c}_k^\dagger(t) \hat{X}_{(\dots)}(t) \rangle$. As usual^{28,29} these correlation functions can be treated as lesser projections of Green functions

$$G_{cX}(\tau, \tau') = -i \langle T_c \hat{c}_k(\tau) \hat{X}_{(\dots)}^\dagger(\tau') \rangle \quad (12)$$

$$G_{Xc}(\tau, \tau') = -i \langle T_c \hat{X}_{(\dots)}(\tau) \hat{c}_k^\dagger(\tau') \rangle \quad (13)$$

respectively, taken at equal time. The last can be obtained by applying Langreth projection rules³⁰ to on-the-contour EOMs for (12) and (13)

$$G_{cX}(\tau, \tau') = \sum_{\mathcal{M}} \int_c d\tau_1 g_k(\tau, \tau_1) V_{k\mathcal{M}} G_{\mathcal{M}, \dots}(\tau_1, \tau') \quad (14)$$

$$G_{Xc}(\tau, \tau') = \sum_{\mathcal{M}} \int_c d\tau_1 G_{\dots, \mathcal{M}}(\tau, \tau_1) V_{\bar{\mathcal{M}}k} g_k(\tau_1, \tau') \quad (15)$$

where $G_{\mathcal{M}, \dots}$ ($G_{\dots, \mathcal{M}}$) is defined in (10), $V_{k\mathcal{M}}$ ($V_{\bar{\mathcal{M}}k}$) is introduced in (9), and

$$g_k(\tau, \tau') \equiv -i \langle T_c c_k(\tau) c_k^\dagger(\tau') \rangle \quad (16)$$

is Green function of free electrons in the contacts.

Using lesser projections taken at equal times of (14) and (15) in (11) leads to (see Appendix A for details)

$$\begin{aligned} \frac{d \langle \hat{X}_{ab}(t) \rangle}{dt} &= i \sum_s \left[H_{ss_a}^{(N_a)} \langle \hat{X}_{(N_a, s; N_b, s_b)}(t) \rangle \right. \\ &\quad \left. - H_{s_b s}^{(N_b)} \langle \hat{X}_{N_a, s_a; N_b, s}(t) \rangle \right] + \sum_{\mathcal{M}, s} \int_{-\infty}^t dt_1 \\ &\quad \left\{ G_{(N_a, s_a; N_b+1, s), \mathcal{M}}^<(t, t_1) \Sigma_{\mathcal{M}, (N_b, s_b; N_b+1, s)}^>(t_1 - t) \right. \\ &\quad + \Sigma_{(N_a, s_a; N_a+1, s), \mathcal{M}}^>(t - t_1) G_{\mathcal{M}, (N_b, s_b; N_a+1, s)}^<(t_1, t) \\ &\quad - G_{(N_a, s_a; N_b+1, s), \mathcal{M}}^>(t, t_1) \Sigma_{\mathcal{M}, (N_b, s_b; N_b+1, s)}^<(t_1 - t) \\ &\quad - \Sigma_{(N_a, s_a; N_a+1, s), \mathcal{M}}^<(t - t_1) G_{\mathcal{M}, (N_b, s_b; N_a+1, s)}^>(t_1, t) \\ &\quad \left. - (-1)^{N_a - N_b} \times \right. \\ &\quad \left[G_{(N_a-1, s; N_b, s_b), \mathcal{M}}^<(t, t_1) \Sigma_{\mathcal{M}, (N_a-1, s; N_a, s_a)}^>(t_1 - t) \right. \\ &\quad + \Sigma_{(N_b-1, s; N_b, s_b), \mathcal{M}}^>(t - t_1) G_{\mathcal{M}, (N_b, s_b; N_a+1, s)}^<(t_1, t) \\ &\quad - G_{(N_a-1, s; N_b, s_b), \mathcal{M}}^>(t, t_1) \Sigma_{\mathcal{M}, (N_a-1, s; N_a, s_a)}^<(t_1 - t) \\ &\quad \left. \left. - \Sigma_{(N_b-1, s; N_b, s_b), \mathcal{M}}^<(t - t_1) G_{\mathcal{M}, (N_b-1, s; N_a, s_a)}^>(t_1, t) \right] \right\} \end{aligned} \quad (17)$$

Here $\Sigma_{\mathcal{M}_1, \mathcal{M}_2}^{>, <}(t)$ are greater and lesser molecular self-energies due to coupling to the contacts

$$\Sigma_{\mathcal{M}_1, \mathcal{M}_2}^{>, <}(t) = \sum_{K=L, R} \Sigma_{\mathcal{M}_1, \mathcal{M}_2}^{(K)>, <}(t) \quad (18)$$

$$\Sigma_{\mathcal{M}_1, \mathcal{M}_2}^{(K)>, <}(t) = \sum_{k \in K} V_{\bar{\mathcal{M}}_1, k} g_k^{>, <}(t) V_{k, \mathcal{M}_2} \quad (19)$$

with $g_k^{>, <}(t)$ being greater and lesser projections of (16)

$$g_k^>(t) = -i[1 - n_k] e^{-i\varepsilon_k t} \quad (20)$$

$$g_k^<(t) = i n_k e^{-i\varepsilon_k t} \quad (21)$$

and $G_{\mathcal{M}_1, \mathcal{M}_2}^{>, <}(t_1, t_2)$ are greater and lesser projections of (10)

$$G_{(a,b), (c;d)}^>(t_1, t_2) = -i \langle \hat{X}_{ab}(t_1) \hat{X}_{cd}^\dagger(t_2) \rangle \quad (22)$$

$$G_{(a,b), (c;d)}^<(t_1, t_2) = \pm i \langle \hat{X}_{cd}^\dagger(t_2) \hat{X}_{ab}(t_1) \rangle \quad (23)$$

Note, in (23) ‘+’ stands when both \mathcal{M}_1 and \mathcal{M}_2 are transitions of Fermi type, and ‘-’ otherwise. For future reference we also define a damping matrix in Liouville space

$$\Gamma_{\mathcal{M}_1, \mathcal{M}_2}^{(K)} \equiv i [\Sigma_{\mathcal{M}_1, \mathcal{M}_2}^> - \Sigma_{\mathcal{M}_1, \mathcal{M}_2}^<] \quad (24)$$

Expression for the current can be derived in a similar way (see Eq.(10) of Ref. 21)

$$\begin{aligned} I_K(t) &= \frac{e}{\hbar} \sum_{\mathcal{M}, \mathcal{M}'} \int_{-\infty}^t dt' \\ &\quad \left\{ \Sigma_{\mathcal{M}, \mathcal{M}'}^<(t - t') G_{\mathcal{M}', \mathcal{M}}^>(t', t) \right. \\ &\quad + G_{\mathcal{M}, \mathcal{M}'}^>(t, t') \Sigma_{\mathcal{M}', \mathcal{M}}^<(t' - t) \\ &\quad - \Sigma_{\mathcal{M}, \mathcal{M}'}^>(t - t') G_{\mathcal{M}', \mathcal{M}}^<(t', t) \\ &\quad \left. - G_{\mathcal{M}, \mathcal{M}'}^<(t, t') \Sigma_{\mathcal{M}', \mathcal{M}}^>(t' - t) \right\} \end{aligned} \quad (25)$$

Equations (17) and (25) are exact, however their right sides are expressed in terms of Green functions. Our goal now is to introduce approximate scheme in order to close (17) in terms of $\langle \hat{X}_{ab}(t) \rangle$, thus finding connection to QME. This approximation is introduced and discussed in the next Section.

III. GENERALIZED QME

Before introduction of an ansatz to close Eq.(17) we note close connection between EOM for $\hat{X}_{ab}(t)$ and density matrix element $\rho_{ba}(t)$. Indeed,

$$\begin{aligned} \rho_{ba}(t) &= \ll \hat{X}_{ba} | e^{-i\mathcal{L}t} | \hat{\rho}_0 \gg = \ll \hat{X}_{ba} | e^{-i\mathcal{L}t} \hat{\rho}_0 \gg \quad (26) \\ &= \ll e^{i\mathcal{L}^\dagger t} \hat{X}_{ba} | \hat{\rho}_0 \gg = \langle \hat{X}_{ab}(t) \rangle \end{aligned}$$

where \mathcal{L} is the total Liouvillian and $\ll A|B \gg \equiv \text{Tr}[\hat{A}^\dagger \hat{B}]$ is scalar product in Liouville space. Hence we expect that Eq.(17) after introducing approximation expressing it in terms of \hat{X}_{ab} only should result in QME.

Correlation function of the type (22) can be *exactly* written in Liouville space as

$$\begin{aligned} &\langle \hat{X}_{ab}(t_1) \hat{X}_{cd}^\dagger(t_2) \rangle = \quad (27) \\ &\quad \theta(t_1 - t_2) \ll \hat{X}_{ba} \hat{I}_K | e^{-i\mathcal{L}(t_1 - t_2)} | \hat{X}_{dc} \hat{\rho}(t_2) \gg \\ &\quad + \theta(t_2 - t_1) \ll \hat{X}_{cd} \hat{I}_K | e^{-i\mathcal{L}(t_2 - t_1)} | \hat{\rho}(t_1) \hat{X}_{ab} \gg . \end{aligned}$$

We introduce the projector superoperator

$$\mathcal{P} = \sum_{ef} | \hat{X}_{ef} \hat{\rho}_K^{eq} \gg \ll \hat{X}_{ef} \hat{I}_K |, \quad (28)$$

which disregards nonequilibrium features in the leads and decouples system and bath dynamics. The ansatz, we propose, replaces (27) by

$$\begin{aligned} < \hat{X}_{ab}(t_1) \hat{X}_{cd}^\dagger(t_2) > \approx & \quad (29) \\ & \theta(t_1 - t_2) \ll \hat{X}_{ba} \hat{I}_K | e^{-i\mathcal{L}(t_1 - t_2)} \mathcal{P} | \hat{X}_{dc} \hat{\rho}(t_2) \gg \\ & + \theta(t_2 - t_1) \ll \hat{X}_{cd} \hat{I}_K | e^{-i\mathcal{L}(t_2 - t_1)} \mathcal{P} | \hat{\rho}(t_1) \hat{X}_{ab} \gg . \end{aligned}$$

Next we introduce retarded and advanced Green functions in the Liouville space (see Appendix B)

$$\begin{aligned} \mathcal{G}_{ij,mn}^r(t) & \equiv -i\theta(t) \ll \hat{X}_{ji} \hat{I}_K | e^{-i\mathcal{L}t} | \hat{X}_{nm} \hat{\rho}_K^{eq} \gg & (30) \\ & = -i\theta(t) \ll \hat{X}_{ji} | \mathcal{U}_{eff}(t) | \hat{X}_{nm} \gg \end{aligned}$$

$$\begin{aligned} \mathcal{G}_{ij,mn}^a(t) & \equiv i\theta(-t) \ll \hat{X}_{mn} \hat{I}_K | e^{i\mathcal{L}t} | \hat{X}_{ij} \hat{\rho}_K^{eq} \gg & (31) \\ & = i\theta(-t) \ll \hat{X}_{ji} | \mathcal{U}_{eff}^\dagger(-t) | \hat{X}_{nm} \gg \end{aligned}$$

where the effective propagator in the molecule space reads

$$\mathcal{U}_{eff} \equiv \ll \cdot \hat{I}_K | e^{-i\mathcal{L}t} | \cdot \hat{\rho}_K^{eq} \gg = \text{Tr}_K \{ e^{-i\mathcal{L}t} \hat{\rho}_K^{eq} \}. \quad (32)$$

Using (30) and (31), we can rewrite (29) as

$$\begin{aligned} & < \hat{X}_{ab}(t_1) \hat{X}_{cd}^\dagger(t_2) > = \\ & i \sum_{e,f} \left[\mathcal{G}_{ab,fe}^r(t_1 - t_2) < \hat{X}_{fe}(t_2) \hat{X}_{cd}^\dagger(t_2) > \right. \\ & \quad \left. - < \hat{X}_{ab}(t_1) \hat{X}_{ef}^\dagger(t_1) > \mathcal{G}_{ef,cd}^a(t_1 - t_2) \right] & (33) \\ & \equiv i \sum_m \left[\mathcal{G}_{ab,md}^r(t_1 - t_2) < \hat{X}_{mc}(t_2) > \right. \\ & \quad \left. - < \hat{X}_{am}(t_1) > \mathcal{G}_{mb,cd}^a(t_1 - t_2) \right] \end{aligned}$$

where second equality follows from orthonormality condition (4).

Similar consideration for correlation function (23) leads to

$$\begin{aligned} & < \hat{X}_{cd}^\dagger(t_2) \hat{X}_{ab}(t_1) > = \\ & i \sum_{e,f} \left[\mathcal{G}_{ab,fe}^r(t_1 - t_2) < \hat{X}_{cd}^\dagger(t_2) \hat{X}_{fe}(t_2) > \right. \\ & \quad \left. - < \hat{X}_{ef}^\dagger(t_1) \hat{X}_{ab}(t_1) > \mathcal{G}_{ef,cd}^a(t_1 - t_2) \right] & (34) \\ & \equiv i \sum_m \left[\mathcal{G}_{ab,cm}^r(t_1 - t_2) < \hat{X}_{dm}(t_2) > \right. \\ & \quad \left. - < \hat{X}_{mb}(t_1) > \mathcal{G}_{am,cd}^a(t_1 - t_2) \right] \end{aligned}$$

It is interesting to note that (33) and (34) can be considered as the Liouville space analog of the generalized Kadanoff-Baym ansatz.²⁵

Using (33) and (34) in (17) closes the latter equation in terms of DM $\rho_{ba}(t) \equiv < \hat{X}_{ab}(t) >$ only

$$\begin{aligned} \frac{d\rho_{12}(t)}{dt} & = -i \sum_{3,4} \left\{ \delta_{N_1, N_3} \delta_{N_2, N_4} \sum_s \left(\delta_{i_2, i_4} H_{i_1, i_3}^{(N_1)} - \delta_{i_1, i_3} H_{i_4, i_2}^{(N_2)} \right) \right. \\ & \quad - i \sum_{s_1, s_2} \int_{-\infty}^{+\infty} dt_1 \left[\mathcal{G}_{(2; N_1+1, s_1)(4; N_3+1, s_2)}^r(t-t_1) \Sigma_{(3; N_3+1, s_2)(1; N_1+1, s_1)}^{<}(t_1-t) \right. \\ & \quad \quad - \Sigma_{(2; N_2+1, s_1)(4; N_4+1, s_2)}^{<}(t-t_1) \mathcal{G}_{(3; N_4+1, s_2)(1; N_2+1, s_1)}^a(t_1-1) \\ & \quad \quad - \mathcal{G}_{(N_2-1, s_1; 1)(N_4-1, s_2; 3)}^r(t-t_1) \Sigma_{(N_4-1, s_2; 4)(N_2-1, s_1; 2)}^{>}(t_1-t) \\ & \quad \quad + \Sigma_{(N_1-1, s_1; 1)(N_3-1, s_2; 3)}^{>}(t-t_1) \mathcal{G}_{(N_3-1, s_2; 4)(N_1-1, s_1; 2)}^a(t_1-t) \\ & \quad \quad - (-1)^{N_1-N_2} \times \left(\mathcal{G}_{(N_2-1, s_1; 1)(4; N_3+1, s_2)}^r(t-t_1) \Sigma_{(3; N_3+1, s_2)(N_2-1, s_1; 2)}^{<}(t_1-t) \right. \\ & \quad \quad - \Sigma_{(N_1-1, s_1; 1)(4; N_4+1, s_2)}^{<}(t-t_1) \mathcal{G}_{(3; N_4+1, s_2)(N_1-1, s_1; 2)}^a(t_1-1) \\ & \quad \quad - \mathcal{G}_{(2; N_1+1, s_1)(N_4-1, s_2; 3)}^r(t-t_1) \Sigma_{(N_4-1, s_2; 4)(1; N_1+1, s_1)}^{>}(t_1-t) \\ & \quad \quad \left. \left. + \Sigma_{(2; N_2+1, s_1)(N_3-1, s_2; 3)}^{>}(t-t_1) \mathcal{G}_{(N_3-1, s_2; 4)(1; N_3+1, s_1)}^a(t_1-t) \right) \right] \times \rho_{34}(t_1) \Big\} & (35) \end{aligned}$$

This is a generalized non-Markovian QME. Note, that

prefactor $(-1)^{N_1-N-2}$ coming from coherences between

different charge blocks is usually lost in the standard QME derivations.

To make (35) more tractable below we assume Markovian generator \mathcal{L}_{eff} (e.g. Markovian Redfield generator^{31,32,34}) for retarded and advanced Green functions (30) and (31)

$$\mathcal{U}_{eff}(t) \approx e^{-i\mathcal{L}_{eff}t}, \quad (36)$$

So that

$$\mathcal{G}_{ij,mn}^r(t) \equiv -i\theta(t) \ll \hat{X}_{ji} | e^{-i\mathcal{L}_{eff}t} | \hat{X}_{nm} \gg \quad (37)$$

$$\mathcal{G}_{ij,mn}^a(t) \equiv i\theta(-t) \ll \hat{X}_{ji} | e^{-i\mathcal{L}_{eff}^\dagger t} | \hat{X}_{nm} \gg. \quad (38)$$

The ansatz (29) together with (37) and (38) is equivalent to use of the regression formula on the Hubbard Green function. This procedure is commonly used to calculate multipoint correlation functions using effective Markovian propagators^{31,32,33}.

The standard non-Markovian QME¹⁶ is obtained from (35) by using in (37) and (38) the free molecular evolution $\mathcal{L}_{\mathcal{M}} = [\hat{H}_M, \cdot]$ instead of the effective one \mathcal{L}_{eff} . Note that difference between standard and generalized versions of QME is similar to dressing of diagrams in GF diagrammatic technique. Note also that the standard QME by itself can not reproduce, e.g., broadening of molecular levels due to coupling to the contacts as noted in Ref. 13.

Below we use the Markovian Redfield equation to get \mathcal{L}_{eff} (see Appendix C). Its spectral decomposition

$$\mathcal{L}_{eff} = \sum_{\gamma} |R_{\gamma} \gg \lambda_{\gamma} \ll L_{\gamma}| \quad (39)$$

with eigenvalues λ_{γ} and left $|L_{\gamma} \gg$ and right $|R_{\gamma} \gg$ eigenvectors, provides a numerically tractable scheme to deal with generalized QME (35) by utilizing

$$\mathcal{G}_{ij,mn}^r(t) = -i\theta(t) \sum_{\gamma} \ll ji | R_{\gamma} \gg e^{-i\lambda_{\gamma}t} \ll L_{\gamma} | nm \gg \quad (40)$$

$$\mathcal{G}_{ij,mn}^a(t) = i\theta(-t) \sum_{\gamma} \ll ji | L_{\gamma} \gg e^{-i\lambda_{\gamma}^*t} \ll R_{\gamma} | nm \gg \quad (41)$$

Steady-state for (35) is given by the right eigenvector with zero eigenvalue of the Liouvillian corresponding to the Markov limit of (35).

Similarly, approximate expression for current in terms

of $\langle \hat{X}_{(\dots)} \rangle$ can be obtained using (33) and (34) in (25)

$$\begin{aligned} I_K(t) &= \frac{e}{\hbar} \sum_{\mathcal{M}_1, \mathcal{M}_2} \sum_e \int_{-\infty}^{+\infty} dt_1 \\ &2\text{Re} \left[\mathcal{G}_{(N_1, i_1; N_1+1, j_1), (N_2, i_2; e)}^r(t-t_1) \right. \\ &\quad \times \Sigma_{(N_2, i_2; N_2+1, j_2), (N_1, i_1; N_1+1, j_1)}^>(t_1-t) \\ &\quad \times \langle \hat{X}_{(N_2+1, j_2; e)}(t_1) \rangle \\ &\quad + \mathcal{G}_{(N_1, i_1; N_1+1, j_1), (e; N_2+1, j_2)}^r(t-t_1) \\ &\quad \times \Sigma_{(N_2, i_2; N_2+1, j_2), (N_1, i_1; N_1+1, j_1)}^<(t_1-t) \\ &\quad \left. \times \langle \hat{X}_{(e; N_2, i_2)}(t_1) \rangle \right] \end{aligned} \quad (42)$$

IV. RESULTS AND DISCUSSION

As a first example we consider a simple resonant level model. One has two charge blocks (occupied and unoccupied level) with one state in each of them: $|0\rangle$ and $|1\rangle$. The molecular Hamiltonian is $\hat{H}_M = |1\rangle \varepsilon_0 \langle 1|$. Current (42) in this case becomes

$$\begin{aligned} I_K(t) &= \frac{ie}{\hbar} \int_{-\infty}^t dt_1 \{ \\ &[\mathcal{G}_{01,01}^r(t-t_1) \Sigma_K^>(t_1-t) - \Sigma_K^>(t-t_1) \mathcal{G}_{01,01}^a(t_1-t)] \\ &\quad \times \rho_{11}(t_1) \\ &+ [\mathcal{G}_{01,01}^r(t-t_1) \Sigma_K^<(t_1-t) - \Sigma_K^<(t-t_1) \mathcal{G}_{01,01}^a(t_1-t)] \\ &\quad \times \rho_{00}(t_1) \} \end{aligned} \quad (43)$$

where

$$\mathcal{G}_{01,01}^r(t) = -i\theta(t) e^{-i(\varepsilon_0 - i\Gamma/2)t} \equiv G^r(t) \quad (44)$$

$$\mathcal{G}_{01,01}^a(t) = i\theta(-t) e^{-i(\varepsilon_0 + i\Gamma/2)t} \equiv G^a(t) \quad (45)$$

and $\Gamma = \sum_{K=L,R} \Gamma_{01,01}^K$ with Γ^K defined in (24). Generalized QME (17) yields

$$\begin{aligned} \frac{d\rho_{11}(t)}{dt} &= -\frac{d\rho_{00}(t)}{dt} = \int_{-\infty}^t dt_1 \{ \\ &[\mathcal{G}_{01,01}^r(t-t_1) \Sigma^>(t_1-t) - \Sigma^>(t-t_1) \mathcal{G}_{01,01}^a(t_1-t)] \\ &\quad \times \rho_{11}(t_1) \\ &+ [\mathcal{G}_{01,01}^r(t-t_1) \Sigma^<(t_1-t) - \Sigma^<(t-t_1) \mathcal{G}_{01,01}^a(t_1-t)] \\ &\quad \times \rho_{00}(t_1) \} \end{aligned} \quad (46)$$

At steady-state (46) yields

$$\rho_{11} = 1 - \rho_{00} = n_0 \quad (47)$$

with n_0 average occupation of the level

$$n_0 = \int_{-\infty}^{+\infty} \frac{dE}{2\pi} A(E) \left[\frac{\Gamma_L}{\Gamma} f_L(E) + \frac{\Gamma_R}{\Gamma} f_R(E) \right] \quad (48)$$

$$A(E) = \frac{\Gamma}{(E - \varepsilon_0)^2 + (\Gamma/2)^2} \quad (49)$$

where $A(E)$ is spectral function and $f_K(E)$ is Fermi distribution in contact $K = L, R$. Using (44), (45), and (47) in (43) leads to the Landauer expression

$$I_K = \frac{e}{\hbar} \int_{-\infty}^{+\infty} \frac{dE}{2\pi} \frac{\Gamma_L \Gamma_R}{\Gamma} A(E) [f_L(E) - f_R(E)] \quad (50)$$

Note, that generalized QME approach takes level broadening into account in a natural way contrary to the standard QME considerations.

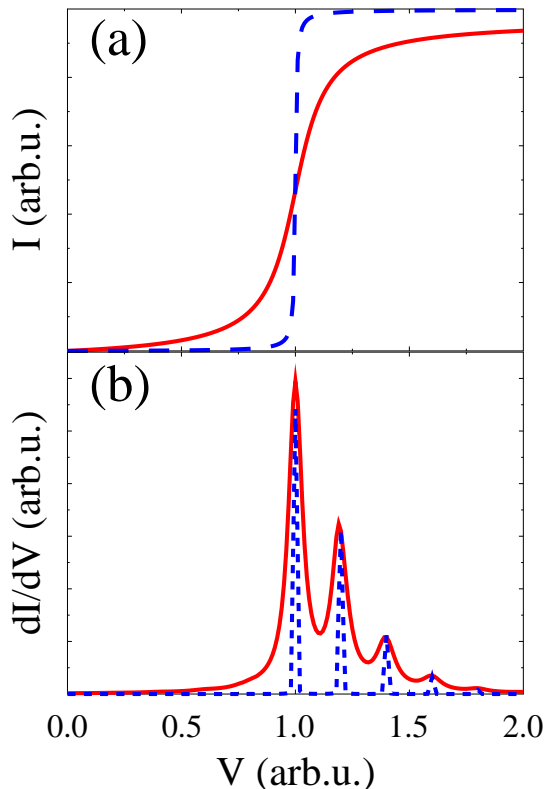


FIG. 1: (Color online) Comparison of generalized (solid line, red) to standard (dashed line, blue) QME results for resonant level model. (a) Current vs. bias for single level. (b) Conductance vs. bias for single level coupled to a vibration. See text for parameters.

Now we present several numerical examples. Figure 1 compares results of calculation within our generalized QME (solid line) and standard QME (dashed line) approaches. Fig. 1a shows current-voltage characteristic of single resonant level ε_0 model. Generalized QME accounts for level broadening due to coupling to the contacts, while standard QME approach misses the broadening altogether. Parameters of the calculation are $\varepsilon_0 = 1$, $\Gamma_L = \Gamma_R = 0.1$, $E_F = \mu_R = 0$, $\mu_L = E_F + |e|V_{sd}$. Here and below we use arbitrary units. Fig. 1b shows conductance vs. bias for the model of single level ε_0 coupled to a vibration ω_0 . Once more, while generalized QME provides reasonable results (compare e.g to Fig.4 of Ref. 18) a

standard QME approach is capable of predicting only positions of the peaks. Parameters of the calculation are $\Gamma_L = \Gamma_R = 0.05$, $\omega_0 = 0.2$, and $M = 0.2$. The last is strength of electron-vibration coupling on the bridge with corresponding Hamiltonian $M(\hat{a} + \hat{a}^\dagger)\hat{n}_0$, where \hat{a}^\dagger (\hat{a}) are creation (annihilation) operators of vibrational quanta and \hat{n}_0 operator of the level population. Other parameters are as in Fig. 1a. Note, that in simulations we used small but finite broadening for the standard QME approach in order to avoid delta-function divergencies in conductance. We also scaled the standard QME result in Fig. 1b for convenience.

Figures 2 present conductance maps for a quantum dot obtained within the generalized QME approach and similar to those obtained within many-body Green function technique (see Ref. 21). Parameters of the calculation are level positions $\varepsilon_\sigma = -0.5$ ($\sigma = \{\uparrow, \downarrow\}$), molecule-contacts coupling $\Gamma_{K,\sigma} = 0.01$ ($K = \{L, R\}$), on-site repulsion $U = 1$, Fermi level $E_F = 0$. Electrochemical potentials in the contacts are $\mu_L = E_F + |e|V_{sd}/2$ and $\mu_R = E_F - |e|V_{sd}/2$. Deviations from this ‘standard’ set for each calculation are specified below. Fig. 2a shows conductance map for QD with level degeneracy removed by e.g. external magnetic field $\varepsilon_\uparrow = -0.6$ and $\varepsilon_\downarrow = -0.4$. For discussion on origin and intensity of peaks see Ref. 35. Fig. 2b shows conductance map for QD coupled to a vibration $\omega_0 = 0.1$ and $M = 0.1$. In addition to resonant peaks vibrational sidebands corresponding to resonant inelastic tunneling are reproduced as well. Fig. 2c shows conductance map for QD with asymmetric coupling to the contacts $\Gamma_{L,\sigma} = 0.01$ and $\Gamma_{R,\sigma} = 0.1$. This result is similar to the one presented in Fig.4 of Ref. 13

Note, that vibrations in both Fig. 1b and 2b were introduced, as is usually done in resonant inelastic transport considerations, with the help of small polaron transformation. So that vibrational features in electron transport stem from the Franck-Condon factors calculated under assumption of unperturbed thermal distribution of vibrational population. Actual vibrational states are not included in the current consideration, and their incorporation into many-body state description will be described elsewhere.

Finally, we consider a model of two-level bridge with coherences in the eigenbasis of the bridge induced by coupling to the contacts. This model was previously considered in Ref. 16 within standard QME approach. Figure 3 presents comparison between standard and generalized QME approaches. Parameters of the calculation are similar to those in Ref. 16 – eigenenergies of the bridge are $\varepsilon_1 = 5\text{eV}$ and $\varepsilon_2\text{eV}$, strength of their coupling to contacts is $T_1^L = T_2^L = 0.3\text{eV}$, $T_1^R = 0.2\text{eV}$, $T_2^R = 0.4\text{eV}$. For temperature we take physically reasonable value of $T = 0.03\text{eV}$. Figures 3a and 3b show current and one of the probabilities (probability of the system to be unoccupied) vs. applied bias. One sees that broadening due to coupling to the contacts is preserved in our scheme. Note, that broadening presented in Ref. 16 was due to unphysically high value of temperature chosen. Fig. 3c

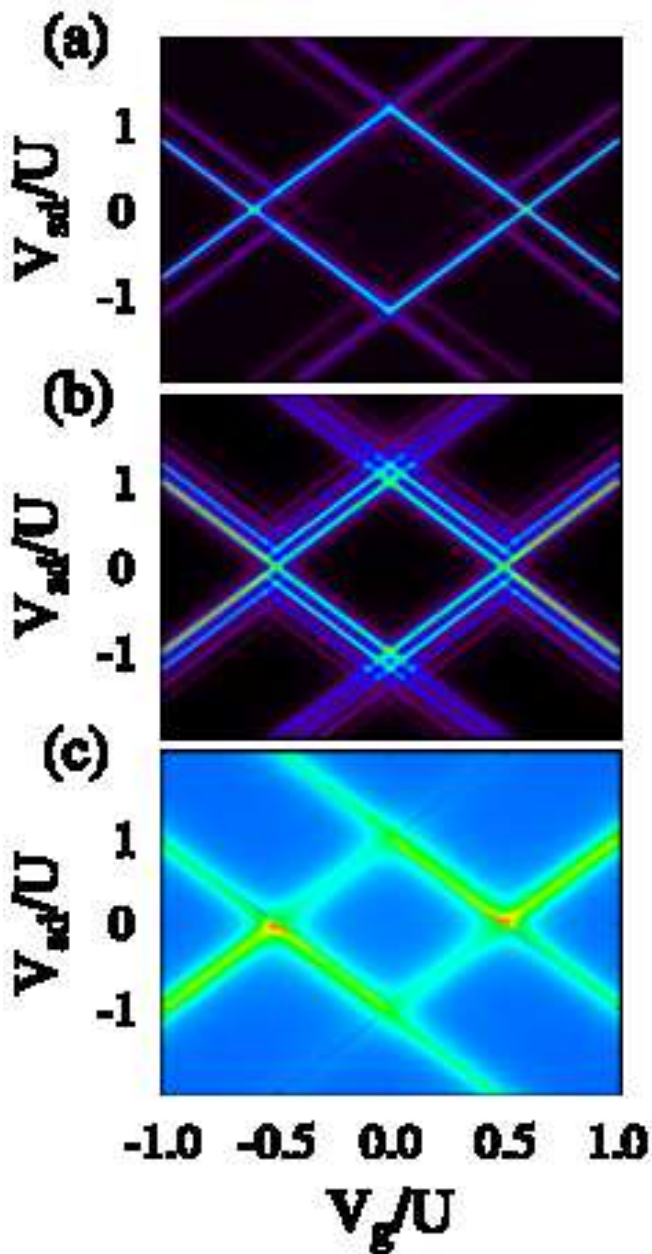


FIG. 2: (Color online) Conductance vs. applied bias V_{sd} and gate voltage V_g for a quantum dot (QD) within generalized QME approach. Shown are results for models of (a) QD with level degeneracy removed (e.g. by applied magnetic field), (b) QD coupled to a vibration, and (c) QD with asymmetric coupling to the contacts. See text for parameters.

demonstrate influence of broadening on coherences (in local basis). Here we bring the two eigenenergies closer to each other, $\varepsilon_1 = 3\text{eV}$, in order to make coherences due to coupling to the contacts more pronounced. One sees that taking level broadening into account changes the coherences essentially.

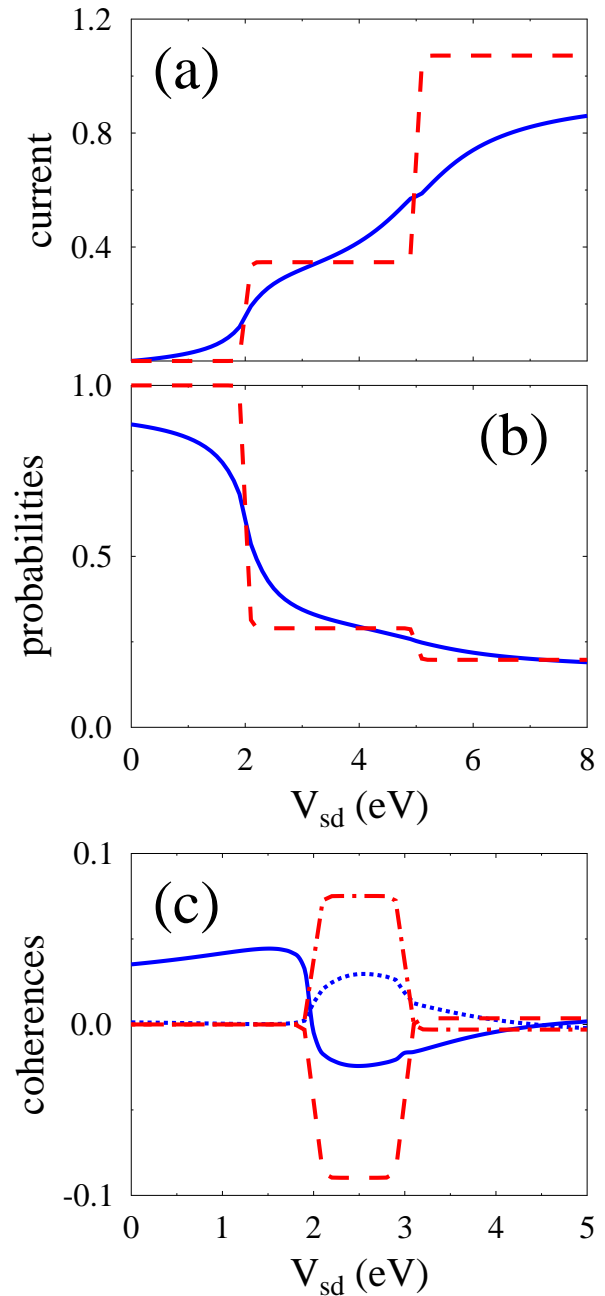


FIG. 3: (Color online) Two-level bridge with coherences in the eigenbasis of the system induced by coupling to contacts.¹⁶ (a) Current and (b) probability for the system to be unoccupied vs. applied bias – generalized (solid line, blue) and standard (dashed line, red) QME considerations. (c) Real (solid, blue and dashed, red) and imaginary (dotted, blue and dash-dotted, red) parts of coherences in the local basis vs. applied bias for generalized and standard QME treatment, respectively. See text for parameters.

V. CONCLUSION

Necessity for description of molecular transport in the language of many-body (isolated molecule) states, essential for description of resonant tunneling and for study of optoelectronic devices, has been realized and several approaches were proposed.^{4,5,6,7,8,9,10,11,19,20,21} Here we introduce a simplified version of the Hubbard operator Green function approach considered in application to inelastic transport in our previous publication.²¹ The simplified approach is formulated for density matrix instead of GF and provides more easy way for calculating both time-dependent and steady state transport in molecular junctions. Starting from GF-type consideration we introduce Liouville space analog of the generalized Kadanoff-Baym ansatz, which allows us to derive generalized QME. The latter differs from the standard QME by incorporating effective propagation in place of free evolution. The procedure is similar in spirit to diagrams dressing in GF diagrammatic techniques. Capabilities of the scheme are demonstrated within model calculations. Application of the approach to opto-electronic response of molecular junctions is a goal for future research.

Acknowledgments

M.E. is funded by the FNRS Belgium (chargé de recherche) and by the Luxembourgish Government (bourse de formation-recherche). M.G. gratefully acknowledges support from the UCSD Startup Fund. This work was performed, in part, at the Center for Integrated Nanotechnologies, a U.S. Department of Energy, Office of Basic Energy Sciences user facility at Los Alamos National Laboratory (Contract DE-AC52-06NA25396).

APPENDIX A: DERIVATION OF EQ.(17)

We start from Eq.(11), which after evaluating the commutator becomes

$$\begin{aligned} \frac{d \langle \hat{X}_{ab}(t) \rangle}{dt} = & -i \left\{ \sum_s \left[H_{s_b, s}^{(N_b)} \langle \hat{X}_{(N_a, s_a; N_b, s)}(t) \rangle \right. \right. \\ & \left. \left. - \langle \hat{X}_{(N_a, s; N_b, s_b)} \rangle H_{s, s_a}^{(N_a)} \right] + \sum_{s, k} [(-1)^{N_a - N_b} \times \right. \\ & \left. \left(V_{k, (N_b, s_b; N_b + 1, s)} \langle \hat{c}_k^\dagger(t) \hat{X}_{(N_a, s_a; N_b + 1, s)}(t) \rangle \right. \right. \\ & \left. \left. - V_{(N_a + 1, s; N_a, s_a), k} \langle \hat{X}_{(N_b, s_b; N_a + 1, s)}^\dagger(t) \hat{c}_k(t) \rangle \right) \right. \\ & \left. + V_{(N_b, s_b; N_b - 1, s), k} \langle \hat{X}_{(N_b - 1, s; N_a, s_a)}^\dagger(t) \hat{c}_k(t) \rangle \right. \\ & \left. \left. - V_{k, (N_a - 1, s; N_a, s_a)} \langle \hat{c}_k^\dagger(t) \hat{X}_{(N_a - 1, s; N_b, s_b)}(t) \rangle \right] \right\} \end{aligned} \quad (\text{A1})$$

where $\sum_s \dots$ is sum over molecular states within charge block, $\sum_k \dots$ is sum over states in the contacts, and fac-

tor $(-1)^{N_a - N_b}$ results from commuting \hat{X}_{ab} with \hat{c}_k (\hat{c}_k^\dagger).

Correlation functions in the right of Eq.(A1) can be identified as lesser projections of the GFs (12) and (13) defined on the Keldysh contour. EOMs for this GFs are presented in (14) and (15). Taking lesser projection of the EOMs and applying the Langreth rules³⁰ yields, e.g. for the first correlation function in (A1)

$$\begin{aligned} & \langle \hat{c}_k^\dagger(t) \hat{X}_{(N_a, s_a; N_b + 1, s)}(t) \rangle \equiv (-1)^{N_a - N_b - 1} i G_{Xc}(t, t) \\ & = (-1)^{N_a - N_b - 1} \sum_{\mathcal{M}} \int_{-\infty}^{+\infty} dt_1 [(-1)^{N_a - N_b - 1} \times \\ & \quad \langle \hat{X}_{\mathcal{M}}^\dagger(t_1) \hat{X}_{(N_a, s_a; N_b + 1, s)}(t) \rangle g_k^a(t_1 - t) \quad (\text{A2}) \\ & \quad + \theta(t - t_1) \left(\langle \hat{X}_{(N_a, s_a; N_b + 1, s)}(t) \hat{X}_{\mathcal{M}}^\dagger(t_1) \rangle \right. \\ & \quad \left. - (-1)^{N_a - N_b - 1} \langle \hat{X}_{\mathcal{M}}^\dagger(t_1) \hat{X}_{(N_a, s_a; N_b + 1, s)}(t) \rangle \right) \\ & \quad \times g_k^<(t_1 - t)] \end{aligned}$$

where $g_k^{a, <}(t)$ are advanced and lesser projections of the GF (16), $\langle \dots \rangle = \text{Tr}[\dots \hat{\rho}_0]$ with initial density matrix taken as usual at infinite past, and where general property of GFs $G^r(t) = \theta(t)[G^>(t) - G^<(t)]$ was used for the G_{XX} GF. Once more factors $(-1)^{N_a - N_b - 1}$ trace Fermi or Bose character of \hat{X}_{ab} . Using $g_k^a(t) = \theta(-t)[g_k^<(t) - g_k^>(t)]$ and utilizing (18) and (19) leads to final expression for the first correlation function in (A1). Repeating consideration for the three other correlation functions in (A1), and using the resulting expressions in (A1) leads to Eq.(17).

APPENDIX B: GREEN FUNCTIONS IN THE LIOUVILLE SPACE

Here we discuss properties of retarded and advanced Green functions in the Liouville space. We start from definitions (30) and (32). Utilizing the property of the full unitary propagator

$$\ll \hat{A} | e^{-i\mathcal{L}t} | \hat{B} \gg = \ll \hat{A}^\dagger | e^{-i\mathcal{L}t} | \hat{B}^\dagger \gg^* \quad (\text{B1})$$

one can write

$$\begin{aligned} \ll \hat{X}_{ij} | \mathcal{U}_{eff}(t) | \hat{X}_{mn} \gg & = \ll \hat{X}_{ji} | \mathcal{U}_{eff}(t) | \hat{X}_{nm} \gg^* \\ & = \ll \hat{X}_{nm} | \mathcal{U}_{eff}^\dagger(t) | \hat{X}_{ji} \gg \quad (\text{B2}) \end{aligned}$$

where the second equality comes from definition of Hermitian conjugate. Using (B2) in (30) one gets

$$\begin{aligned} \mathcal{G}_{ij, mn}^a(t) & = \mathcal{G}_{mn, ij}^{r*}(-t) \\ & = i\theta(-t) \ll \hat{X}_{mn} | \mathcal{U}_{eff}(-t) | \hat{X}_{ij} \gg \quad (\text{B3}) \end{aligned}$$

Note, that definitions (30) and (31) lead to the usual Hermitian-type connection (B3) between retarded and advance Green functions $\mathcal{G}^a = [\mathcal{G}^r]^\dagger$. An alternative def-

inition

$$\mathcal{G}_{ij,mn}^r(t) \equiv -i\theta(t) \ll \hat{X}_{ji} \hat{I}_K | e^{-i\mathcal{L}t} | \hat{X}_{mn} \hat{\rho}_K^{eq} \gg \quad (\text{B4})$$

$$= -i\theta(t) \ll \hat{X}_{ji} | \mathcal{U}_{eff}(t) | \hat{X}_{mn} \gg$$

$$\mathcal{G}_{ij,mn}^a(t) \equiv i\theta(-t) \ll \hat{X}_{nm} \hat{I}_K | e^{i\mathcal{L}t} | \hat{X}_{ij} \hat{\rho}_K^{eq} \gg \quad (\text{B5})$$

$$= i\theta(-t) \ll \hat{X}_{ji} | \mathcal{U}_{eff}^\dagger(-t) | \hat{X}_{mn} \gg$$

would lead to Liouvillian conjugation³⁶ $\mathcal{G}^a = [\mathcal{G}^r]^\times$ or

$$\mathcal{G}_{ij,mn}^a(t) = \mathcal{G}_{nm,ji}^{r*}(-t) \quad (\text{B6})$$

APPENDIX C: EXPRESSION FOR \mathcal{L}_{eff}

We start from (37) and (38) and use free propagator in place of effective one. This leads to

$$\mathcal{G}_{ij,mn}^{(0)r}(t) = -i\theta(t) \ll \hat{X}_{ji} | e^{-i\mathcal{L}_M t} | \hat{X}_{nm} \gg \quad (\text{C1})$$

$$\equiv -i\theta(t) \langle j | e^{-i\hat{H}_M t} | n \rangle \langle m | e^{i\hat{H}_M t} | i \rangle$$

$$\mathcal{G}_{ij,mn}^{(0)a}(t) = i\theta(-t) \ll \hat{X}_{ji} | e^{-i\mathcal{L}_M^\dagger t} | \hat{X}_{nm} \gg \quad (\text{C2})$$

$$\equiv i\theta(-t) \langle j | e^{-i\hat{H}_M t} | n \rangle \langle m | e^{i\hat{H}_M t} | i \rangle$$

Substituting (C1) and (C2) into (35) and using standard Markov approximation

$$\rho_{ab}(t_1) \approx \sum_{c,d} \ll ab | e^{i\mathcal{L}_M(t-t_1)} | cd \gg \rho_{cd}(t) \quad (\text{C3})$$

one gets the (Markovian) Redfield quantum master equation

$$\frac{d\rho_{ab}(t)}{dt} = -i \sum_{c,d} \ll ab | \mathcal{L}_{eff} | cd \gg \rho_{cd}(t),$$

where the generator for our model takes the form

$$\begin{aligned} -i\mathcal{L}_{(a;b),(c;d)}^{eff} &= i\mathcal{L}_{(b;a),(d;c)}^{eff\dagger} = -i \left\{ \delta_{N_a, N_c} \delta_{N_b, N_d} \left[H_{s_a, s}^{(N_a)} \delta_{s_b, s_d} - \delta_{s_a, s_c} H_{s_d, s_b}^{(N_b)} \right] - \frac{1}{2} \sum_{i,j} \sum_{p,r} \right. \\ & \left[\delta_{N_a+1, N_c} \delta_{N_b+1, N_d} (-1)^{N_a - N_b} \times \right. \\ & \left(U_{ri}^{(N_a+1)} U_{sc_i}^{*(N_a+1)} U_{s_a j}^{(N_a)} U_{pj}^{*(N_a)} \Sigma_{(N_b, s_b; N_b+1, s_d), (N_a, p; N_a+1, r)}^> (E_i^{(N_a+1)} - E_j^{(N_a)}) \right. \\ & \left. \left. + U_{s_d i}^{(N_b+1)} U_{ri}^{*(N_b+1)} U_{pj}^{(N_b)} U_{s_b j}^{*(N_b)} \Sigma_{(N_b, p; N_b+1, r), (N_a, s_a; N_a+1, s_c)}^> (E_i^{(N_b+1)} - E_j^{(N_b)}) \right) \right. \\ & - \delta_{N_a-1, N_c} \delta_{N_b-1, N_d} (-1)^{N_a - N_b} \times \\ & \left(U_{s_a i}^{(N_a)} U_{ri}^{*(N_a)} U_{pj}^{(N_a-1)} U_{s_c j}^{*(N_a-1)} \Sigma_{(N_a-1, p; N_a, r), (N_b-1, s_d; N_b, s_b)}^< (E_i^{(N_a)} - E_j^{(N_a-1)}) \right. \\ & \left. \left. + U_{ri}^{(N_b)} U_{s_b i}^{*(N_b)} U_{s_d j}^{(N_b-1)} U_{pj}^{*(N_b-1)} \Sigma_{(N_a-1, s_c; N_a, s_a), (N_b-1, p; N_b, r)}^< (E_i^{(N_b)} - E_j^{(N_b-1)}) \right) \right. \\ & \left. + \delta_{N_a, N_c} \delta_{N_b, N_d} \delta_{s_a, s_c} \right. \\ & \sum_s \left(U_{ri}^{(N_b+1)} U_{si}^{*(N_b+1)} U_{s_d j}^{(N_b)} U_{pj}^{*(N_b)} \Sigma_{(N_b, s_b; N_b+1, s), (N_b, p; N_b+1, r)}^< (E_i^{(N_b+1)} - E_j^{(N_b)}) \right. \\ & \left. \left. - U_{s_d i}^{(N_b)} U_{ri}^{*(N_b)} U_{pj}^{(N_b-1)} U_{sj}^{*(N_b-1)} \Sigma_{(N_b-1, p; N_b, r), (N_b-1, s; N_b, s_b)}^> (E_i^{(N_b)} - E_j^{(N_b-1)}) \right) \right. \\ & \left. + \delta_{N_a, N_c} \delta_{N_b, N_d} \delta_{s_b, s_d} \right. \\ & \sum_s \left(U_{si}^{(N_a+1)} U_{ri}^{*(N_a+1)} U_{pj}^{(N_a)} U_{s_c j}^{*(N_a)} \Sigma_{(N_a, p; N_a+1, r), (N_a, s_a; N_a+1, s)}^< (E_i^{(N_a+1)} - E_j^{(N_a)}) \right. \\ & \left. \left. - U_{ri}^{(N_a)} U_{s_c i}^{*(N_a)} U_{sj}^{(N_a-1)} U_{pj}^{*(N_a-1)} \Sigma_{(N_a-1, s; N_a, s_a), (N_a-1, p; N_a, r)}^> (E_i^{(N_a)} - E_j^{(N_a-1)}) \right) \right) \left. \right\} \end{aligned} \quad (\text{C4})$$

where $\mathbf{U}^{(N)}$ are unitary transformations diagonalizing charge blocks $\mathbf{H}_M^{(N)}$ of the molecular Hamiltonian (7),

and $E_i^{(N)}$ are corresponding eigenvalues.

-
- * Also at Center for Nonlinear Phenomena and Complex Systems, Université Libre de Bruxelles, Code Postal 231, Campus Plaine, B-1050 Brussels, Belgium
- ¹ M.Galperin, M.A.Ratner, A.Nitzan, and A.Troisi, *Science* **319**, 1056 (2008).
 - ² D.R.Ward, N.J.Halas, J.W.Ciszek, J.M.Tour, Y.Wu, P.Nordlander, and D.Natelson, *Nano Lett.* **8**, 919 (2008).
 - ³ J.Bonca and S.A.Trugman, *Phys. Rev. Lett.* **75**, 2566 (1995).
 - ⁴ B.Muralidharan, A.W.Ghosh, and S.Datta, *Phys. Rev. B* **73**, 155410 (2006).
 - ⁵ L.Siddiqui, A.W.Ghosh, and S.Datta, *Phys. Rev. B* **76**, 085433 (2007).
 - ⁶ J.Koch and F. von Oppen, *Phys. Rev. Lett.* **94**, 206804 (2005).
 - ⁷ J.Koch, F. von Oppen, and A.V.Andreev, *Phys. Rev. B* **74**, 205438 (2006).
 - ⁸ J.Koch, M.E.Raikh, and F. von Oppen, *Phys. Rev. Lett.* **96**, 056803 (2006).
 - ⁹ J.Koch, E.Sela, Y.Oreg, and F. von Oppen, *Phys. Rev. B* **75**, 195402 (2007).
 - ¹⁰ E.G.Petrov, V.May, and P.Hänggi, *Chem. Phys.* **319**, 380 (2005).
 - ¹¹ E.G.Petrov, V.May, and P.Hänggi, *Phys. Rev. B* **73**, 045408 (2006).
 - ¹² H.Schoeller, *Lecture Notes in Physics* **544**, 137 (2000).
 - ¹³ J.N.Pedersen and A.Wacker, *Phys. Rev. B* **72**, 195330 (2005).
 - ¹⁴ X.Q.Li, J.Luo, Y.G.Yang, P.Cui, and Y.J.Yan, *Phys. Rev. B* **71**, 205304 (2005).
 - ¹⁵ S.Welack, M.Schreiber, and U.Kleinekathferb, *J. Chem. Phys.* **124**, 044712 (2006).
 - ¹⁶ U.Harbola, M.Esposito and S.Mukamel, *Phys. Rev. B* **74**, 235309 (2006).
 - ¹⁷ A.Mitra, I.Aleiner, and A.J.Millis, *Phys. Rev. B* **69**, 245302 (2004).
 - ¹⁸ M.Galperin, A.Nitzan, and M.A.Ratner, *Phys. Rev. B* **73**, 045314 (2006).
 - ¹⁹ I.Sandalov, B.Johansson, and O.Eriksson, *Int. J. Quant. Chem.* **94**, 113 (2003).
 - ²⁰ J.Fransson, *Phys. Rev. B* **72**, 075314 (2005).
 - ²¹ M.Galperin, A.Nitzan, and M.A.Ratner, *Phys. Rev. B* **78**, 125320 (2008).
 - ²² See footnote [51] in Ref. 21. M.G. thanks Tomáš Novotný for helpful discussion.
 - ²³ J.N.Pedersen, D.Bohr, A.Wacker, T.Novotný, P.Schmitteckert, and K.Flensberg. arXiv:0810:5293 (2008).
 - ²⁴ I.V.Ovchinnikov and D.Neuhauser, *J. Chem. Phys.* **122**, 024707 (2005).
 - ²⁵ H.Haug and A.Jauho, *Quantum Kinetics in Transport and Optics of Semiconductors*, Springer-Verlag (1996).
 - ²⁶ J.Fransson, O.Eriksson, and I.Sandalov, *Phys. Rev. B* **66**, 195319 (2002).
 - ²⁷ M.Galperin and S.Tretiak, *J. Chem. Phys.* **128**, 124705 (2008).
 - ²⁸ Y.Meir and N.S.Wingreen, *Phys. Rev. Lett.* **68**, 2512 (1992).
 - ²⁹ A.P.Jauho, N.S.Wingreen, and Y.Meir, *Phys. Rev. B* **50**, 5528 (1994).
 - ³⁰ D.C.Langreth, p.3-32 in *Linear and Nonlinear Electron Transport in Solids*, edited by J.T.Devreese and D. E. Doren, Plenum Press: New York, (1976).
 - ³¹ H.-P.Breuer and F.Petruccione, *The Theory of Open Quantum Systems*, Oxford University Press: Oxford (2002).
 - ³² C.W.Gardiner and P.Zoller, *Quantum noise*, 2nd ed., Springer: Berlin (2000).
 - ³³ H.J.Carmichael, *Statistical Methods in Quantum Optics 1*, Springer: Berlin (1999).
 - ³⁴ R.Kubo, M.Toda, and N.Hashitsume, *Statistical Physics II: Nonequilibrium Statistical Mechanics*, 2nd ed., Springer: Berlin (1998).
 - ³⁵ M.Galperin, A.Nitzan, M.A.Ratner, *Phys. Rev. B* **76**, 035301 (2007).
 - ³⁶ A.Ben-Reuven and S.Mukamel, *J. Phys. A: Math. Gen.* **8**, 1313 (1975).